Multidisciplinary Sciences, Volume 16. (2026) No. 4, pp. 15–31. *https://doi.org/10.35925/j.multi.2026.4.2*

INFLUENCE-MATRIX ACCELERATION OF RANDOM-WALK-BASED PCB TEMPERATURE DISTRIBUTION RECONSTRUCTION

Árpád Gábor Móré[*] and Attila Trohák

University of Miskolc, 3515 Miskolc, Hungary
[*] *Corresponding author*
{arpad.more, attila.trohak}@uni-miskolc.hu

Abstract. The temperature distribution developed during the reflow soldering process strongly influences solder joint quality, component thermal loading, and the reliability of electronic assemblies. Local temperature variations may lead to soldering defects, incomplete wetting, overheating, and long-term reliability problems. In industrial practice, however, the PCB temperature is typically available only at a limited number of measurement locations, usually seven points. Consequently, reconstructing the complete temperature distribution from sparse measurement data is of considerable practical importance. In our previous research, a Random Walk (RW)-based model was developed for reconstructing the complete temperature distribution. Although the model provides satisfactory reconstruction accuracy, each new measurement state requires repeated stochastic simulations, resulting in significant computational effort. This paper presents an influence-matrix formulation of the RW model that expresses the temperature reconstruction as a linear operator. The proposed approach incorporates the PCB geometry, topology, and measurement-point arrangement into a precomputed influence matrix. Consequently, under unchanged industrial measurement conditions, the temperature distribution can be reconstructed by a single matrix-vector multiplication instead of repeated stochastic simulations. The method was evaluated on a 10 × 15 cell PCB model using seven measurement points. For 500 random walks, the conventional RW model required 0.25828 s, whereas the influence-matrix approach reconstructed the temperature field in 0.00018 s, corresponding to a 1434.89-fold speed-up. Leave-one-out validation confirmed that the proposed method preserves the reconstruction accuracy of the original RW model while reducing the computational time for repeated evaluations by several orders of magnitude.

Keywords: Random Walk; Influence Matrix; Temperature-Field Reconstruction; Printed Circuit Board; Reflow Soldering.

1 Introduction

The quality of surface-mounted electronic assemblies is fundamentally affected by the temperature-time profile developed during reflow soldering. An appropriate profile ensures complete melting and wetting of the solder while limiting the thermal load imposed on components, the substrate, and the solder joints. In practice, therefore, knowledge of the oven's set zone temperatures alone is insufficient; it is also necessary to determine the planar temperature distribution that develops across a printed circuit board (PCB) containing regions with different heat capacities and thermal conductivities. The industrial importance of temperature profiling is emphasized by the IPC-7530 guideline [1], while the spatially and temporally varying heat-transfer conditions in convection reflow ovens constitute a complex modelling problem in their own right [2-4].

Direct measurement of the entire PCB surface in a production environment is limited for several reasons. The number of thermocouples is finite, their attachment may influence the measurement results, and wiring and data acquisition increase experimental complexity. Infrared thermography is also subject to uncertainties arising from variations in emissivity, occlusion, limited optical access, and the enclosed design of the oven. Consequently, reconstruction methods capable of estimating temperatures at unmeasured locations from a limited number of

reliable measurement points are required [5-7]. Such methods must be numerically accurate, physically interpretable, repeatable, and sufficiently fast for industrial applications.

In our previous work, a stochastic Random Walk (RW)-based reconstruction model was developed to determine the temperature distribution of printed circuit boards from a limited number of measurement points [8]. In this method, a random walk starts from a cell with unknown temperature and continues until it reaches a measurement point with a known temperature. The relative frequencies of the endpoints obtained from a large number of independent walks determine the probability that the walk terminates at each measurement point. These absorption probabilities serve as weighting factors for the reconstructed temperature, which is obtained as a weighted combination of the measured temperatures. The method is based on the probabilistic interpretation of the discrete Laplace equation; consequently, the weighting factors are not merely numerical coefficients but also represent the physical and probabilistic properties of the heat-transfer process [9-12].

A limitation of the direct Random Walk procedure is that the random walks must be repeated whenever a new temperature state is evaluated. However, for a fixed PCB geometry and an unchanged measurement-point layout, the trajectories of the walks are determined solely by the geometry, topology, boundary conditions, and the locations of the measurement points; they are independent of the measured temperature values. Consequently, the absorption probabilities remain unchanged. These probabilities therefore need to be determined only once and stored in an influence matrix that can subsequently be reused for every new measurement state. As a result, reconstruction of the complete temperature field is reduced to a single matrix-vector multiplication.

The objective of this study is to derive mathematically, describe algorithmically, and evaluate computationally the influence-matrix formulation of the previously developed Random Walk model. The investigation addresses three questions: (i) how the Random Walk reconstruction can be formulated as a linear operator; (ii) to what extent the computational time can be reduced by constructing the influence matrix only once; and (iii) after how many repeated evaluations the computational cost of constructing the influence matrix is recovered.

The novelty of this study is the explicit formulation of the absorption probabilities as a reusable, row-normalized influence matrix. The proposed mathematical formulation preserves the physical and probabilistic interpretation of the Random Walk method while separating the geometry-dependent weighting factors from the measured temperature values. Consequently, repeated temperature-field reconstruction can be performed by a single matrix-vector multiplication. The study also investigates the conditions under which the one-time computational cost of constructing the influence matrix is recovered in repeated industrial temperature-field evaluations.

2 Theoretical Background and Previous Research

This section outlines the Random Walk (RW)-based reconstruction method and the computational characteristics that motivate its acceleration. It then examines which parts of the computation depend on the PCB configuration and which vary with the measured temperatures.

2.1 Random-Walk-Based Reconstruction

In our previous work, a Random Walk (RW)-based model was developed for reconstructing the temperature distribution of printed circuit boards from a limited number of temperature measurements [8]. The model reconstructs the temperature field by describing the relationship between measured and unmeasured locations through a stochastic process.

For every cell with an unknown temperature, a large number of independent random walks are initiated. At an interior cell, each walk moves to one of the four edge-connected neighbouring cells with equal probability (0.25). At the domain boundary, steps leading outside the computational domain are not permitted; therefore, the transition probabilities are renormalized over the remaining accessible neighbouring cells. Consequently, every walk remains within the computational domain throughout the simulation. Measurement points represent absorbing states, and each walk terminates immediately after reaching the first measurement point.

The endpoint of a single random walk is inherently random; therefore, one walk alone is insufficient to characterize the relationship between the starting cell and the measurement points. By performing a sufficiently large number of independent walks, the relative frequency with which the walks terminate at each measurement point can be estimated. These relative frequencies represent the absorption probabilities that characterize the relationship between the starting cell and the individual measurement points and provide the basis for reconstructing the complete temperature field.

The reconstruction accuracy of the RW model was validated in our previous work using leave-one-out validation [13], [8]. The present study builds upon this previously validated reconstruction model and examines its computational structure with particular emphasis on the repeated computations required for successive measurement states when the PCB geometry and the measurement-point configuration remain unchanged.

In the RW calculation, the transition rules are determined by the domain geometry, cell connectivity, boundary treatment, measurement-point locations, and the random-number sequence used. The measured temperatures enter the calculation only after a walk has terminated, when values assigned to the endpoints are weighted. It follows that, for an unchanged model configuration, the $p_k(i,j)$ weights need not be regenerated for every new technological state [14].

The practical importance of this reusability is particularly high in reflow profiling [15]. A single PCB with the same sensor layout can be examined under different oven settings, conveyor speeds, product variants, or profile time points. The direct RW algorithm repeats the stochastic simulation for every measurement state, whereas the proposed influence-matrix formulation separates the geometry-dependent computation from the measured temperature values. Consequently, the influence matrix is constructed only once and subsequently reused for all repeated reconstructions, substantially reducing the computational effort while preserving the probabilistic foundation of the RW method.

The research gap is therefore not the absence of a new physical model for the complete heat-conduction problem but the underuse of the computational structure of the established stochastic reconstruction. The influence matrix formalizes this structure, makes the cell-level weights storable and verifiable, and permits an exact evaluation of the speedup that also accounts for the initial investment cost. The approach requires the geometry, topology, measurement points, and transition rules to remain unchanged within the validity range of the matrix.

2.2 Computational Characteristics of the Random Walk Model

The reconstruction accuracy of the Random Walk (RW) model was demonstrated in our previous work. However, the computational effort of the method may become significant when the complete temperature field has to be reconstructed for a large number of measurement states. During the reconstruction process, a large number of random walks are initiated from every cell with an unknown temperature and continue until a measurement point is reached. This procedure is repeated for every cell within the computational domain.

The computational cost depends primarily on three factors: the number of cells in the computational grid, the number of random walks initiated from each cell, and the average walk length. Increasing the grid resolution increases the number of starting cells, while increasing the number of walks reduces statistical uncertainty at the expense of additional computation. The average walk length depends mainly on the geometry of the computational domain and the spatial arrangement of the measurement points.

In practical reflow profiling, temperature fields are typically reconstructed for a sequence of measurement states corresponding to different process conditions or different time instants of the same thermal profile. Under these conditions, the PCB geometry, computational grid, and measurement-point layout remain unchanged; only the measured temperature values differ from one state to another. Nevertheless, the conventional Random Walk algorithm performs the complete stochastic simulation again for every new measurement state.

This observation raises an important question: Is it really necessary to repeat the same random walks whenever only the measured temperatures change, or can part of the computation be reused while the geometry and measurement-point configuration remain unchanged?

2.3 Analysis of the Computational Structure of the Random Walk Model

The Random Walk model described in the previous section performs the same stochastic procedure for every new measurement state. For each unknown cell, the prescribed number of random walks is generated under identical geometric conditions, using the same transition rules and the same measurement-point configuration.

A closer examination of the algorithm reveals that the trajectories of the random walks are independent of the measured temperature values. During the simulation, a random walk is affected only by the geometry of the computational domain, the connectivity of the cells, the boundary treatment, and the locations of the absorbing measurement points. The walk terminates when a measurement point is reached, regardless of the temperature assigned to that point. Consequently, the stochastic part of the computation is independent of the measured temperatures.

For repeated evaluations performed on the same PCB geometry and with an unchanged measurement-point configuration, only the measured temperature values vary from one state to another. This observation suggests that the stochastic component of the Random Walk model may be separated from the temperature-dependent part of the computation. Such a separation would allow the results of the random walks to be reused without repeating the stochastic simulation for every new measurement state.

The following section presents a mathematical formulation based on this observation.

3 Materials and Methods

This section describes the PCB and measurement configuration used in the evaluation and analyses the Random Walk computation. It then presents the influence-matrix formulation, its construction, and the procedure for reconstructing the temperature field.

3.1 PCB and Measurement Configuration

The method was evaluated using a representation of an approximately 100 mm × 150 mm rectangular printed circuit board (PCB). The PCB surface was represented by a regular grid of 10 rows and 15 columns, resulting in 150 computational cells. This computational grid defines the domain of the Random Walk model and provides a consistent representation of the measurement locations, the starting positions of the random walks, and the reconstructed temperature field. Throughout this study, all Random Walk simulations and subsequent calculations were performed on this computational grid. In Figure 1, the computational cells are identified by the coordinate pair (i, j), where the row index (i) increases from top to bottom and the column index (j) increases from left to right.

Eight Class 1 K-type thermocouples were used in the original industrial measurement setup. Thermocouple No. 1 measured the temperature inside the reflow oven and was not attached to the PCB. Therefore, its measured value did not represent the PCB surface temperature and was not used in the temperature-field reconstruction. The other seven thermocouples were attached to the PCB and retained their original identifiers, No. 2–8, to ensure consistency with the original measurement dataset. Consequently, the PCB measurement points are numbered from 2 to 8 in Table 1 and Figure 1. The nominal measurement accuracy of the thermocouples was ±1.5 °C over the investigated temperature range. The seven PCB measurement points cover 4.67% of the 150 computational cells; consequently, the reconstruction is based on sparse spatial sampling. The temperature vector used in the computational examples corresponds to process state 3 and contains values between 241 °C and 250 °C. The coordinates of the measurement points and the corresponding measured temperatures are summarized in Table 1.

Table 1. *Grid coordinates of the surface-temperature measurement points and values measured in the investigated state.*

Point	Row, i	Column, j	T_k [°C]	Role
2	9	1	250	measurement point

Point	Row, i	Column, j	T_k [°C]	Role
3	3	14	242	measurement point
4	3	6	246	measurement point
5	1	9	243	measurement point
6	6	9	241	measurement point
7	9	13	242	measurement point
8	2	3	243	measurement point

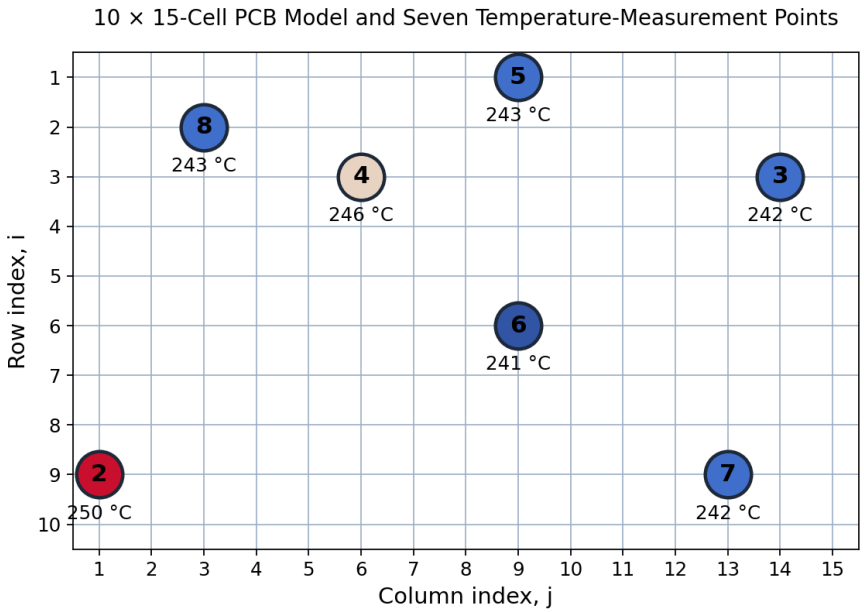

Figure 1. *Locations of the seven surface-measurement points in the 10 × 15-cell model. The numbers inside the circles identify the measurement points.*

The measurement points do not form a regular sampling grid but were selected to represent thermally characteristic locations on the PCB. Their spatial distribution provides information from different regions of the computational domain while preserving a sparse measurement configuration representative of industrial practice. The PCB geometry, computational grid, and measurement-point layout remain unchanged throughout the investigation and therefore define the computational configuration used by the Random Walk model.

3.2 Analysis of the Random Walk Computation

For every starting cell, the Random Walk model determines how frequently the random walks terminate at each measurement point by performing a large number of independent walks. As a result, every starting cell is characterized by a set of probabilities describing the relative frequencies with which the walks terminate at the individual measurement points.

A detailed analysis of the computation shows that these probabilities depend exclusively on the geometry of the computational domain, the connectivity of the computational grid, the boundary treatment, the locations of the measurement points, and the number of simulated random walks. The measured temperature values do not

influence the trajectories of the random walks. During the simulation, the random walk uses only the locations of the measurement points, and the walk terminates as soon as the first measurement point is reached.

When another process state or another point of the thermal profile is evaluated, the PCB geometry, the computational grid, the measurement-point layout, and the transition rules remain unchanged. Only the measured temperatures associated with the measurement points are modified. Consequently, the probabilities obtained from the Random Walk computation are determined repeatedly, although the computational conditions remain identical.

This observation indicates that the geometry-dependent part of the Random Walk computation can be separated from the part that depends on the measured temperatures. The following section presents the mathematical formulation based on this observation.

3.3 Influence Matrix Formulation

The influence matrix describes the probabilistic relationship between every computational cell of the PCB model and the individual temperature-measurement points. Each row of the matrix corresponds to one computational cell, while each column corresponds to one measurement point. The element W_{qk} represents the probability that a Random Walk starting from computational cell (q) terminates at measurement point (k). In the numerical implementation, this probability is estimated from the relative frequency with which the simulated walks reach the individual measurement points.

These probabilities are determined by the PCB geometry, the topology and connectivity of the computational grid, the boundary treatment, the locations of the measurement points, and the transition rules of the Random Walk. They are independent of the temperature values assigned to the measurement points. Consequently, when the model configuration and measurement-point arrangement remain unchanged, the same influence matrix can be reused for different measured temperature vectors. With a finite number of Random Walks, the computed matrix is a stochastic estimate of the underlying absorption probabilities and may vary slightly with the random-number sequence; however, the underlying probability structure remains unchanged.

Let $n_k(i,j)$ denote the number of random walks initiated from computational cell (i,j) that terminate at measurement point k, and let Kdenote the total number of simulated random walks. The corresponding influence coefficient is defined as

$$W_k(i,j) = \frac{n_k(i,j)}{K} \tag{1}$$

where $W_k(i,j)$ represents the probability that a random walk starting from cell (i,j) terminates at measurement point k.

Using linear indexing of the computational cells $(q = 1, \dots, N)$, the influence coefficients are arranged into the influence matrix $W \in \mathbb{R}^{N\times m}$,

$$W_{qk} = \frac{n_{qk}}{K} \tag{2}$$

where N is the total number of computational cells and $m$is the number of measurement points.

Since every random walk terminates at exactly one measurement point, the influence coefficients satisfy

$$W_{qk} \geq 0;\ \sum_{k=1}^{m} W_{qk} = 1,\ \ q = 1, \dots, N \tag{3}$$

The temperature field is reconstructed by multiplying the influence matrix by the measured temperature vector,

$$T = WT_m \tag{4}$$

where T is the reconstructed temperature vector and $T_m$contains the measured temperatures.

Table 2 illustrates the construction of one row of the influence matrix for computational cell (6,5) using 500 random walks. The table presents the number of walks terminating at each measurement point, the corresponding influence coefficients, and their contribution to the reconstructed temperature.

3.4 Construction of the Influence Matrix

The influence matrix is constructed by performing the Random Walk simulation once for the selected computational configuration. Starting from each computational cell, K random walks are generated according to the transition rules described in Section 2. Each random walk is terminated when it reaches one of the measurement points.

For every computational cell, the number of random walks terminating at each measurement point is counted. These termination frequencies are converted into influence coefficients according to (1), and the coefficients are assembled into the corresponding row of the influence matrix using (2). Repeating this procedure for all computational cells yields the complete influence matrix.

Table 2. *Construction of the influence-matrix row for cell (6,5) using K=500 walks.*

Point	**T_k [°C]**	**n_k**	**$W_k(6,5)$**	**$T_k \cdot W_k$ [°C]**
2	250	103	0.206	51.500
3	242	12	0.024	5.808
4	246	112	0.224	55.104
5	243	23	0.046	11.178
6	241	114	0.228	54.948
7	242	35	0.070	16.940
8	243	101	0.202	49.086
Total	-	500	1.000	244.564

Once the influence matrix has been constructed, it can be reused for every subsequent reconstruction, provided that the PCB geometry, computational grid, boundary conditions, measurement-point locations, and the number of simulated random walks remain unchanged. Consequently, each new temperature field is obtained simply by multiplying the precomputed influence matrix by the measured temperature vector according to (4), eliminating the need to repeat the Random Walk simulation for every measurement state.

3.5 Computational Procedure

Once the influence matrix has been constructed, reconstruction of a new temperature field no longer requires repeated Random Walk simulations. Instead, the reconstruction is performed using the precomputed influence matrix and the measured temperature vector.

The computational procedure begins by acquiring the temperatures at the measurement points and assembling them into the measurement vector T_m. The reconstructed temperature field is then obtained by multiplying the influence matrix by the measurement vector according to (4). The overall computational workflow is illustrated in Figure 2.

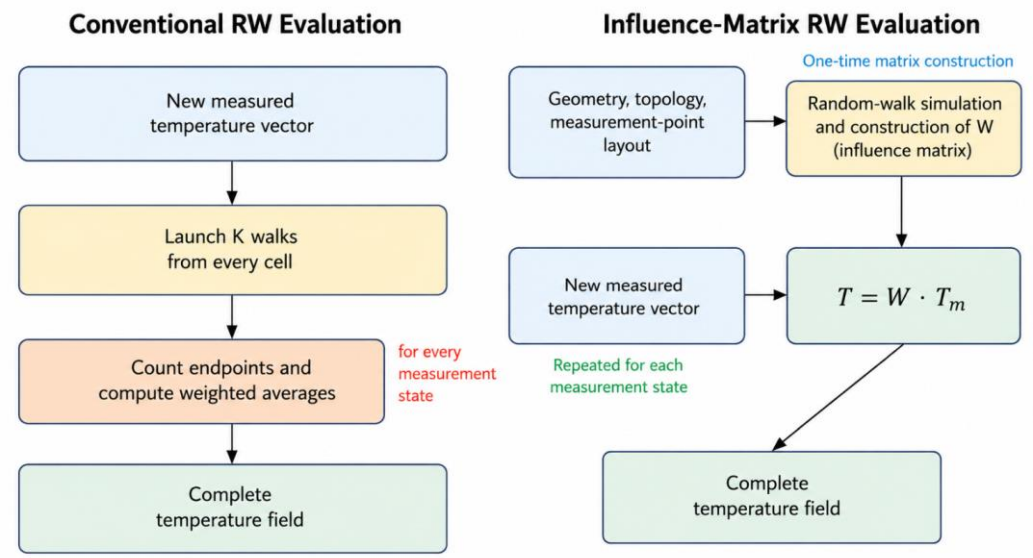

Figure 2. *Comparison of the conventional Random Walk reconstruction and the proposed influence-matrix-based reconstruction procedure.*

The influence matrix is generated only once for the selected computational configuration and stored for subsequent use. For each new measurement state, only the measurement vector is updated, while the same influence matrix is reused to reconstruct the temperature distribution. Consequently, the computational cost of repeated reconstructions is significantly reduced, since the Random Walk simulation is replaced by a single matrix multiplication.

4 Results

This section evaluates the effects of the number of random walks on reconstruction accuracy and runtime, reports the leave-one-out validation, and examines the properties of the influence matrix. It also compares computational performance and determines the break-even point for repeated reconstructions.

4.1 Effect of the Number of Walks on Accuracy and Runtime

For each investigated value of K, the Random Walk calculation was repeated 100 times using a different random-number sequence in every execution. The reconstructed temperature obtained for each computational cell was averaged over these 100 independent realizations. The RMSE values reported in Table 3 were subsequently calculated from the resulting ensemble-averaged temperature field. Therefore, the reported RMSE values characterize the convergence of the mean Random Walk reconstruction rather than the seed-to-seed variability of individual executions.

Increasing the number of walks improved the reconstruction accuracy of the Random Walk model. The RMSE decreased from 0.25 °C at K=100 to 0.10 °C at K=500, with intermediate values of 0.17 °C, 0.14 °C, and 0.12 °C for K=200, 300, and 400, respectively. The improvement became progressively smaller as the number of walks increased, indicating convergence of the Random Walk approximation. This behaviour is consistent with the square-root convergence of random-walk estimates.

Table 3. *Convergence and mean runtime of the RW model based on 100 independent realizations for each value of K.*

K [walks/cell]	RW runtime [s]	RMSE [°C]
100	0.04188	0.25
200	0.08398	0.17
300	0.12723	0.14
400	0.18965	0.12
500	0.21109	0.10

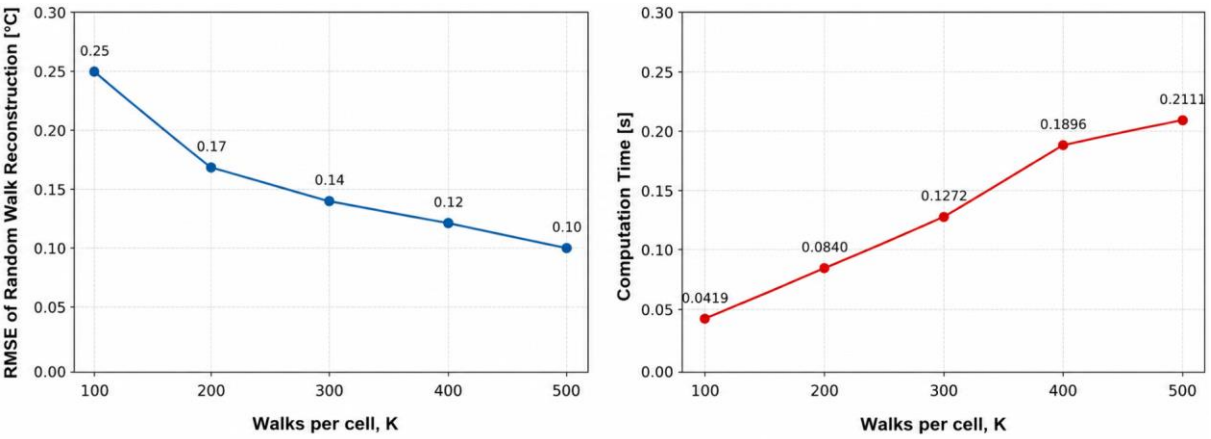

Figure 3. *Effect of the Number of Random Walks on Reconstruction Accuracy and Computation Time.*

Figure 3 shows the relationship between the number of random walks, the reconstruction accuracy, and the computation time. As the number of random walks increases, the RMSE decreases, while the computation time increases approximately linearly. The most significant improvement in reconstruction accuracy is achieved with the first few hundred random walks, whereas further increases provide progressively smaller improvements.

Based on these results, 500 random walks were selected for the subsequent investigations. This value provides a favourable compromise between reconstruction accuracy and computational cost, since additional random walks produce only minor improvements while requiring proportionally longer computation times.

4.2 Leave-One-Out Validation

For validation against measured data, the value of one selected sensor was removed from the input, and the temperature at the omitted location was then estimated from the remaining measurement points. This procedure was performed for the five non-extreme measurement points, namely points 3, 4, 5, 7, and 8. Measurement points 2 and 6 were retained in the validation input because they correspond to the maximum and minimum measured temperatures, respectively. Since every reconstructed value is a convex combination of the retained measurements, the method satisfies the maximum principle and cannot produce a value outside the temperature range of the input vector. Omitting either extreme point would therefore convert the test from interpolation to extrapolation and impose a one-sided constraint on the estimated value. Each omission changes the set of absorbing points; therefore, the random walks for a given validation configuration were evaluated using the corresponding reduced set of measurement points. The objective was not to calibrate individual sensors but to determine how accurately the spatial reconstruction could recover an unknown local temperature from the remaining measurements. The individual leave-one-out estimates and reconstruction errors are presented in Table 4, while the corresponding summary error metrics are provided in Table 5.

Table 4. *Leave-one-out validation results (ΔT = T_estimated − T_measured).*

Omitted point	Coordinate	Measured T [°C]	Estimated T [°C]	ΔT [°C]
3	(3,14)	242.00	242.54	0.54
4	(3,6)	246.00	243.38	−2.62
5	(1,9)	243.00	242.42	−0.58
7	(9,13)	242.00	242.25	0.25
8	(2,3)	243.00	243.96	0.96

Table 5. *Summary metrics of the leave-one-out validation.*

Metric	Value [°C]	Interpretation
Mean signed error	−0.29	slight mean underestimation
MAE	0.99	typical absolute deviation
RMSE	1.30	metric sensitive to larger errors
MaxAE	2.62	largest individual deviation

In four of the five validation cases, the absolute reconstruction error remained below 1 °C. The largest deviation (−2.62 °C) occurred at measurement point 4, indicating a local thermal characteristic that could not be fully reconstructed from the remaining sparse measurement points. The overall performance of the proposed method is characterized by a mean signed error of −0.29 °C, an MAE of 0.99 °C, and an RMSE of 1.30 °C [1].

The leave-one-out validation indicates that the reconstruction accuracy is primarily limited by the sparse spatial distribution of the measurement points and by the simplifying assumptions of the thermal model. Consequently, further increasing the number of random walks is expected to provide only limited improvement in the prediction of measured temperatures, since the dominant source of error arises from the available measurement information rather than from the numerical implementation of the Random Walk method.

4.3 Properties of the Influence Matrix

Every row of the influence matrix is a nonnegative unit-sum weight vector. The operation in Equation (5) therefore preserves a constant field: if every measurement point has the same temperature T_0, every reconstructed cell also has temperature T_0. The same property ensures the maximum principle: no element of the estimated field can be below the measured minimum or above the measured maximum. For the investigated input vector of 241-250 °C, the entire field consequently remains within this interval.

The equivalence of direct RW and influence-matrix RW can be demonstrated algebraically. For computational cell q, the temperature obtained by the original Random Walk method is

$$T_q = \sum_{k=1}^{m} \frac{n_{qk}}{K} T_k \tag{5}$$

where n_{qk} is the number of random walks terminating at measurement point k, and K is the total number of simulated random walks.

Using the definition of the influence coefficients:

$$W_k = \frac{n_{qk}}{K}. \tag{6}$$

Substituting Equation (6) into Equation (5) yields:

$$T_q = \sum_{k=1}^{m} W_{qk} T_k \tag{7}$$

The equivalence between the direct Random Walk calculation and the influence-matrix formulation holds separately for every individual Random Walk realization. A different random-number sequence may produce slightly different endpoint frequencies and, consequently, slightly different influence coefficients. However, when both formulations use the same endpoint frequencies, they produce exactly the same reconstructed temperature values. Therefore, random-seed variability affects the stochastic approximation of the coefficients but does not affect the mathematical equivalence between the original and influence-matrix formulations.

Therefore, the influence-matrix formulation is mathematically identical to the original Random Walk reconstruction. The matrix is therefore a lossless rearrangement of the information obtained from the random walks rather than a new interpolation procedure.

At the same time, the precomputed influence matrix retains the sampling variability associated with the finite number of random walks. This provides a reproducibility advantage, since every subsequent measurement vector produces the same deterministic reconstruction when the same influence matrix is used. If a larger number of random walks is used during construction of the influence matrix, or if several independently generated matrices are averaged, the sampling uncertainty of the weights can be further reduced. Consequently, the reconstruction accuracy can be adjusted by selecting an appropriate number of random walks during construction of the influence matrix.

4.4 Computational Performance

The runtimes of the original RW calculation, the one-time construction of the influence matrix, and the subsequent matrix-vector multiplication were compared for K = 100, 200, and 500. For each investigated value of K, the computational-time measurements were repeated 100 times. The runtime values reported in Table 6 represent the arithmetic means of these 100 executions and were used to reduce the influence of short-term timing fluctuations. The construction time of the influence matrix ranged from 0.04203 to 0.20906 s and was therefore, as expected, of the same order of magnitude as one original RW calculation. In contrast, reconstruction by matrix-vector multiplication required 0.00016–0.00023 s and did not increase with K, because K affects only the accuracy of the constructed influence matrix, whereas the dimensions of the stored W matrix remain unchanged.

Table 6. *Mean computation times for the direct and influence-matrix RW methods based on 100 executions.*

K	Original RW [s]	Construction of W [s]	$T=W\cdot T_m$ [s]	Speedup
100	0.04227	0.04203	0.00016	264.19×
200	0.08602	0.08664	0.00023	374.00×
500	0.25828	0,21109	0.00018	1,434.89×

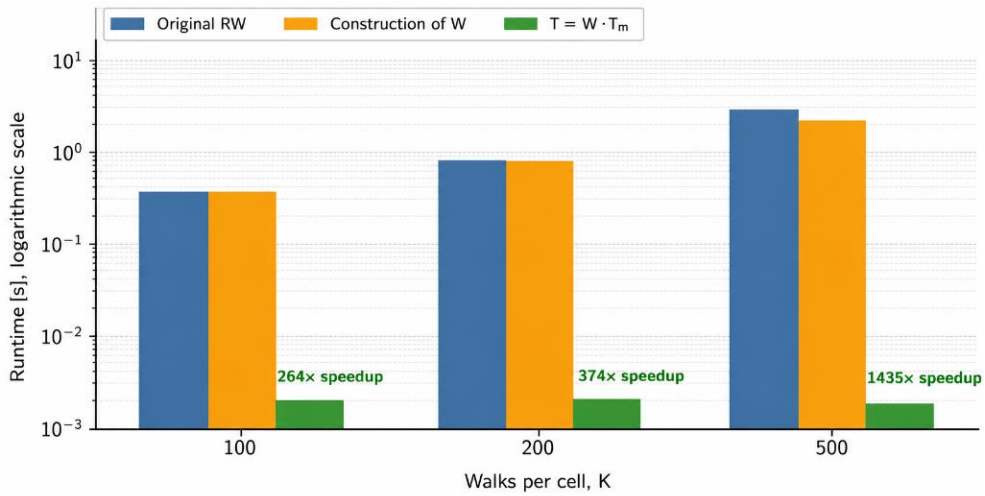

Figure 4. *Comparison of the computation times of the original RW method, influence-matrix construction, and matrix-vector multiplication.*

The computational speedup was 264.19-fold at K = 100, 374.00-fold at K = 200, and 1,434.89-fold at K = 500. The speedup increases because the computational cost of the original RW method grows with K, whereas the computational cost of the matrix-vector multiplication depends only on the dimensions of the influence matrix. For K = 500, the measured runtime of 0.00018 s is sufficiently short that timer resolution, the VBA environment, and operating-system scheduling may have a noticeable influence on the measured value. Therefore, the reported speedup should be interpreted as an experimental result obtained for the present implementation rather than as a universal constant.

The matrix-vector multiplication uses the same influence matrix constructed with the selected value of K; consequently, the reconstruction accuracy obtained during construction of the influence matrix is preserved for all subsequent temperature reconstructions. The computationally intensive stage is therefore performed only once during construction of the influence matrix.

4.5 Amortized Cost and Break-Even Point

The reported speedup considers only the repeated reconstruction stage and does not include the one-time cost of constructing the influence matrix. For a single measurement state, the appropriate comparison is therefore between the direct RW computation and the total computation required by the influence-matrix approach. At K = 100, the total matrix-based time is 0.04219 s, slightly lower than the direct computation time of 0.04227 s. At K = 200, the corresponding values are 0.08687 s and 0.08602 s, respectively, indicating a marginal additional cost for the first reconstruction. At K = 500, the total matrix-based computation requires 0.20924 s, already providing a 1.23-fold advantage over the direct RW computation even for a single measurement state. The amortized speedup values calculated for different numbers of measurement states are summarized in Table 7.

Table 7. *Amortized speedup of the influence-matrix procedure as a function of the number of states*

K	M=1	M=10	M=100	Asymptotic speedup
100	1.002×	9.69×	72.79×	264.19×
200	0.990×	9.69×	78.49×	374.00×
500	1.234×	12.25×	113.75×	1,434.89×

The values for M = 1, 10, and 100 represent the total amortized speedup, including the one-time influence-matrix construction.

The dependence of the amortized speedup on the number of evaluated measurement states is illustrated in Figure 5.

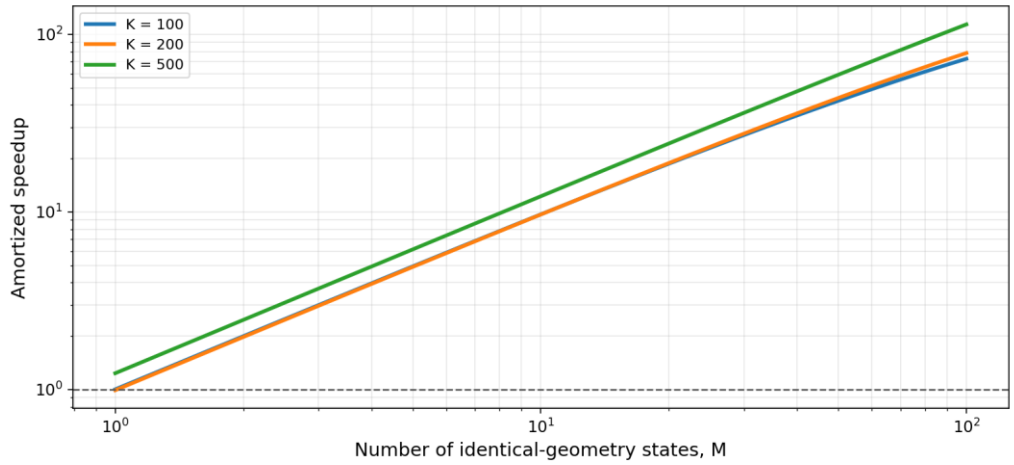

Figure 5. *Amortized speedup as a function of the number of measurement states evaluated on the same geometry.*

For ten measurement states, the amortized speedup is nearly one order of magnitude for every investigated value of K: 9.69× for $K = 100$ and $K = 200$, and 12.25× for $K = 500$. For 100 measurement states, the corresponding values increase to 72.79×, 78.49×, and 113.75×, respectively. As the number of measurement states increases, the amortized speedup approaches the asymptotic speedup because the one-time cost of constructing the influence matrix is distributed over an increasing number of temperature reconstructions.

Based on the measured runtimes, the influence-matrix approach becomes clearly advantageous from the second evaluated state onward for K = 200. For K = 100 and K = 500, the total computational cost of the influence-matrix approach is already lower for the first evaluated state, although at K = 100 the difference is comparable to the timing uncertainty. Therefore, under the investigated conditions, the one-time cost of constructing the influence matrix is recovered after one or two evaluations, and each additional state further increases the computational benefit.

5 Discussion

This section interprets the influence-matrix formulation and relates it to deterministic numerical methods. It also discusses reconstruction accuracy, practical applicability, the method's limitations, and directions for further research.

5.1 Scientific Interpretation

The principal contribution of this study is not the computational speedup itself but the reformulation of the Random Walk (RW) reconstruction as a reusable linear operator. The stochastic simulation depends only on the PCB geometry, computational topology, boundary treatment, and measurement-point configuration, whereas the measured temperatures influence only the final linear combination of the precomputed absorption probabilities. This separation makes it possible to construct an influence matrix that completely characterizes the spatial response of the investigated configuration.

The proposed formulation transforms the original stochastic reconstruction into a two-stage procedure. The computationally demanding influence-matrix construction is performed only once, while each subsequent temperature reconstruction is reduced to a deterministic matrix-vector multiplication. The resulting computational

speedup is therefore not achieved through numerical approximation but follows directly from the mathematical separation of the geometry-dependent and temperature-dependent components of the reconstruction process.

The influence matrix also provides a physically interpretable representation of the reconstruction. Each row contains the probabilities that a random walk initiated from a given computational cell reaches the individual measurement points. Consequently, the matrix preserves the probabilistic interpretation of the original RW model while providing a compact and reusable description of the relationship between sparse measurements and the reconstructed temperature field.

5.2 Relation to Deterministic Numerical Methods

The discrete Laplace equation underlying the present Random Walk model can also be solved using deterministic numerical methods, including the finite difference method (FDM), the finite element method (FEM), and direct linear algebra. On a regular computational grid, FDM produces a sparse system of linear equations whose solution provides the discrete temperature field. Direct linear algebra can solve this system deterministically and therefore does not introduce the sampling variability associated with a finite number of Random Walks. FEM offers greater flexibility for irregular geometries, heterogeneous material properties, and more complex boundary conditions, although it requires the construction of an appropriate finite-element mesh and system matrices.

The objective of the present study is not to introduce a new general method for solving the Laplace equation or to demonstrate superiority over established deterministic solvers. Instead, the study addresses the repeated computational effort of the previously developed and validated Random Walk reconstruction method. The proposed influence-matrix formulation preserves the original Random Walk model and its probabilistic interpretation while avoiding the repetition of the stochastic simulation for every new measured temperature vector. Therefore, the computational evaluation is deliberately restricted to comparing the original Random Walk implementation with its influence-matrix-based acceleration under identical geometry, measurement-point arrangement, transition rules, and computational conditions. A quantitative comparison with independently implemented FEM and FDM solvers would require harmonized discretization, boundary conditions, numerical tolerances, and implementation environments and is considered a separate subject for future investigation.

5.3 Reconstruction Accuracy and Measurement Information

The reconstruction accuracy is governed primarily by the amount and spatial distribution of the available measurement information rather than by the numerical implementation of the Random Walk algorithm. Increasing the number of random walks reduces the stochastic sampling uncertainty; however, beyond approximately 500 walks, the improvement becomes marginal. Under these conditions, additional computational effort provides only limited gains in reconstruction accuracy.

The leave-one-out validation demonstrates that the reconstruction quality is mainly limited by the sparse measurement configuration and the simplified thermal representation of the PCB. With only seven measurement points available, a considerable part of the temperature field must be estimated from indirect information. Consequently, further improvements in reconstruction accuracy are expected to result primarily from optimized sensor placement or more detailed physical modelling rather than from increasing the number of simulated random walks [17].

The proposed influence-matrix formulation preserves the reconstruction accuracy of the original Random Walk model while eliminating repeated stochastic simulations. Therefore, the accuracy of the reconstructed temperature field remains determined principally by the quality of the available measurement information, whereas the influence-matrix formulation substantially improves computational efficiency without altering the underlying physical interpretation of the reconstruction process.

5.4 Practical Applicability

The proposed influence-matrix formulation is particularly advantageous in industrial applications where the PCB geometry and the measurement-point configuration remain unchanged while multiple temperature states must be

evaluated. Under these conditions, the influence matrix is constructed only once and subsequently reused for every new measurement state, reducing the reconstruction to a single matrix-vector multiplication.

This approach is well suited for repeated evaluation of reflow soldering profiles, including different oven settings, conveyor speeds, or production batches. The substantial reduction in computational time enables rapid reconstruction of complete temperature fields without compromising reconstruction accuracy.

The methodology is not limited to PCB temperature reconstruction. The same computational principle can be applied to other boundary-value problems in which the geometry remains fixed while the measured boundary conditions vary, making the influence-matrix formulation applicable to a broader class of engineering reconstruction problems.

5.5 Limitations and Validity Range

The proposed influence-matrix formulation is valid only when the PCB geometry, computational grid, boundary conditions, and measurement-point configuration remain unchanged. Any modification of these parameters requires reconstruction of the corresponding influence matrix.

The present investigation is based on a two-dimensional steady-state thermal model with isotropic four-directional random walks. Consequently, effects such as transient heat transfer, internal heat generation, multilayer PCB structures, and temperature-dependent material properties are not explicitly represented. These simplifications should be considered when applying the method to more complex thermal systems.

Furthermore, the experimental validation was performed using a single PCB configuration with seven measurement points. Although the results demonstrate the effectiveness of the proposed approach, additional investigations involving different PCB geometries, measurement configurations, and operating conditions are required to further establish its general applicability.

The present study focuses on the ensemble-averaged convergence and computational acceleration of the previously validated Random Walk method. It does not provide a separate statistical characterization of the seed-to-seed distribution of the individual Random Walk realizations. Such an analysis, including confidence intervals calculated from individually stored results and inferential statistical testing, would require a different data-recording procedure and is considered a subject for future investigation.

5.6 Directions for Further Research

Future research should focus on extending the proposed methodology to more complex PCB geometries, including non-rectangular domains and multilayer structures, as well as incorporating additional physical phenomena such as transient heat transfer and internal heat generation.

Another important direction is the optimization of measurement-point placement. Since the influence matrix explicitly describes the contribution of each measurement point to the reconstructed temperature field, it provides a suitable basis for selecting sensor locations that maximize reconstruction accuracy while minimizing the number of required measurements.

Finally, the influence-matrix concept may be extended beyond PCB temperature reconstruction to other engineering problems involving repeated evaluation of boundary-value systems with fixed geometry and varying measurement data. This offers opportunities for applying the proposed methodology in a broader range of thermal and diffusion-related reconstruction problems.

6 Conclusions

This study presented an influence-matrix formulation of the Random Walk method for reconstructing PCB temperature distributions from sparse measurement data. The principal contribution is the recognition that the stochastic reconstruction can be separated into a geometry-dependent component and a temperature-dependent linear component. This enables the construction of a reusable influence matrix that transforms repeated stochastic simulations into a simple matrix-vector multiplication.

The proposed formulation preserves the reconstruction accuracy and physical interpretation of the original Random Walk method while substantially reducing the computational effort required for repeated evaluations.

The greatest benefit is achieved in applications where multiple temperature fields must be reconstructed for an unchanged PCB geometry and measurement-point configuration.

The presented methodology provides an efficient and physically interpretable framework for temperature-field reconstruction from limited measurement data. Beyond PCB temperature analysis, the proposed influence-matrix concept may also be applicable to other engineering problems involving repeated evaluation of boundary-value systems with fixed geometry and varying measured boundary conditions.

Author Contributions: Conceptualization, M.Á.G.; methodology, M.Á.G.; software, M.Á.G.; validation, M.Á.G. and T.A.; formal analysis, M.Á.G. and T.A.; investigation, M.Á.G.; resources, M.Á.G.; data curation, M.Á.G.; writing-original draft preparation, M.Á.G.; writing-review and editing, M.Á.G. and T.A.; visualization, M.Á.G.; supervision, T.A.; project administration, M.Á.G. Both authors have read and approved the version of the manuscript intended for submission.

Conflicts of Interest: The authors declare no conflict of interest related to the preparation or publication of this study.

Declaration of Generative AI Use: During preparation of this manuscript, the authors used OpenAI ChatGPT for language improvement, support with text organization, and editorial assistance. The authors reviewed all generated and modified content in full, verified the numerical data and references, and accept sole responsibility for the published content.

Abbreviations

The abbreviations used throughout the manuscript are summarized in Table 8.

Table 8. *Abbreviations used in the manuscript*

Abbreviation	Definition
AI	Artificial Intelligence
MAE	Mean Absolute Error
PCB	Printed Circuit Board
RMSE	Root Mean Square Error
RW	Random Walk
VBA	Visual Basic for Applications

References

[1] IPC. IPC-7530:2025 Guidelines for Temperature Profiling for Mass Soldering Processes (Reflow & Wave). IPC, 2025.

[2] Illés, B. Distribution of the heat transfer coefficient in convection reflow oven. *Applied Thermal Engineering*, 2010, 30(13), 1523–1530. https://doi.org/10.1016/j.applthermaleng.2010.02.016

[3] Illés, B. Measuring heat transfer coefficient in convection reflow ovens. *Measurement*, 2010, 43(9), 1134–1141. https://doi.org/10.1016/j.measurement.2010.05.004

[4] Bozsóki, I., Géczy, A., Illés, B. Overview of different approaches in numerical modelling of reflow soldering applications. *Energies*, 2023, 16(16), 5856. https://doi.org/10.3390/en16165856

[5] Móré, Á. G., Trohák, A. Modelling the temperature distribution of printed circuit boards (In Hungarian). *Multidiszciplináris Tudományok*, 2022, 12(1), 71–78. https://doi.org/10.35925/j.multi.2022.1.6

[6] Móré, Á. G., Trohák, A., Vásárhelyi, J. Modeling temperature distribution using a mathematical method. In: 24th International Carpathian Control Conference (ICCC), IEEE, 2023, 294–298. https://doi.org/10.1109/ICCC57093.2023.10178903

[7] Wang, W., Yu, B., Ai, Q., Liu, M., Shuai, Y., Wang, X., Zhang, X. Reconstructing 3D temperature fields from sparse discrete data by analytical solution-embedded neural network. *Applied Thermal Engineering*, 2025, 264, 125448. https://doi.org/10.1016/j.applthermaleng.2025.125448

[8] Móré, Á. G., Trohák, A., Vásárhelyi, J. Intelligent computational method for temperature distribution. *Pollack Periodica: An International Journal for Engineering and Information Sciences*, 2026. Online First. https://doi.org/10.1556/606.2025.01427

[9] Dumka, P., Chauhan, R., Mishra, R., Dave, D., Sonawane, C., Pandey, A., Tejani, G. Modelling two-dimensional Laplace equation using Monte Carlo simulation: A Python viewpoint. *Mathematical Modelling of Engineering Problems*, 2025, 12(1), 159–165. https://doi.org/10.18280/mmep.120118

[10] Grigoriu, M. A Monte Carlo solution of heat conduction and Poisson equations. *Journal of Heat Transfer*, 2000, 122(1), 40–45. https://doi.org/10.1115/1.521435

[11] Révész, P. Random Walk in Random and Non-Random Environments. World Scientific, Singapore, 1990. https://doi.org/10.1142/1107

[12] Talebi, S., Gharehbash, K., Jalali, H. R. Study on random walk and its application to solution of heat conduction equation by Monte Carlo method. *Progress in Nuclear Energy*, 2017, 96, 18–35. https://doi.org/10.1016/j.pnucene.2016.12.004

[13] Móré, Á. G., Trohák, A., Vásárhelyi, J. Comparison of modeled and measured temperature distribution values (In Hungarian). In: Doktoranduszok Fóruma, Miskolci Egyetem, 2024, 79–83.

[14] Milewski, S. Recovery of thermal load parameters by means of the Monte Carlo method with fixed and meshless random walks. *Applied Mathematics in Science and Engineering*, 2022, 30(1), 1–40. https://doi.org/10.1080/17415977.2021.2016738

[15] Móré, Á. G., Trohák, A., Vásárhelyi, J. Production optimization by modeling temperature distribution (In Hungarian). In: XXVI. Tavaszi Szél Konferencia, 2023, 473–480.

[16] Chai, T., Draxler, R. R. Root mean square error (RMSE) or mean absolute error (MAE)? Arguments against avoiding RMSE in the literature. *Geoscientific Model Development*, 2014, 7, 1247–1250. https://doi.org/10.5194/gmd-7-1247-2014

[17] Liu, X., Yao, W., Peng, W., Fu, Z., Xiang, Z., Chen, X. A physics-driven sensor placement optimization methodology for temperature field reconstruction. *Applied Thermal Engineering*, 2024, 257, 124476. https://doi.org/10.1016/j.applthermaleng.2024.124476